# Transparent nonlinear optical crystallized glass fibers with highly oriented Ba2TiGe208 crystals



doi: 10.1063/1.2890144

# Transparent nonlinear optical crystallized glass fibers with highly oriented $Ba_2TiGe_2O_8$ crystals

Yosuke Hane,[1] Takayuki Komatsu,[1,a)] Yasuhiko Benino,[2] and Takumi Fujiwara[3]
[1]*Department of Materials Science and Technology, Nagaoka University of Technology, 1603-1 Kamitomioka-cho, Nagaoka 940-2188, Japan*
[2]*Department of Material and Energy Science, Graduate School of Environmental Science, Okayama University, 3-1-1 Tsushima-Naka, Okayama 700-8530, Japan*
[3]*Department of Applied Physics, Graduate School of Engineering, Tohoku University, 6-6-05 Aoba, Sendai 980-8579, Japan*

(Received 17 September 2007; accepted 29 December 2007; published online 21 March 2008)

Glass fibers with a diameter of 100–200 $\mu$m are drawn by just pulling up melts of $30BaO-15TiO_2-55GeO_2$ glass, and transparent crystallized glass fibers consisting of nonlinear optical $Ba_2TiGe_2O_8$ crystals are fabricated by crystallization of glass fibers. It is clarified from linearly polarized micro-Raman scattering spectra that fibers show the surface crystallization and $Ba_2TiGe_2O_8$ crystals grow from the surface to the interior, giving *c*-axis orientations. It is found that holes are formed frequently in the center of fully crystallized glass fibers, and transparent hollow crystallized glass fibers are fabricated through careful heat treatments, e.g., fibers with $\phi=200$ $\mu$m show hollows (capillary-type holes) with $\phi=40$ $\mu$m. By adding a small amount of $Sb_2O_3$ in glass fiber preparations, transparent crystallized glass fibers with no holes are developed and second harmonic generations (SHGs) are clearly observed from such fibers. The present study proposes that transparent crystallized glass fibers showing strong SHGs would have a potential for fiber-type light control optical devices. © *2008 American Institute of Physics*.
[DOI: 10.1063/1.2890144]

## I. INTRODUCTION

Fiber-type devices with active functions for optical signal processing such as modulation and routing are one of the most promising components in the new era of all fiber network systems. Optical fiber exhibiting electro-optic effect or second-order optical nonlinearity is an attractive candidate because these properties allow the realization of the above active functions. A lot of efforts for the fabrication of single-crystal fibers using nonlinear optical crystals such as $LiNbO_3$ have been spent so far.[1] However, considering that the present telecommunication network systems have been constructed by the so-called silica glass fibers, glass-related fibers with active functions would be favorable for applications in fiber network systems. As glass has random structure with inversion symmetry in atomic arrangements, generation of active functional properties such as ferroelectricity or second-order optical nonlinearity arising from anisotropic atomic arrangements cannot be expected in glass, in principle. We need, therefore, to develop glass-related fibers including ferroelectrics or nonlinear optical crystals without loosing optical transparency.

There have been many reports on the fabrication of transparent crystallized glasses (glass ceramics) consisting of ferroelectrics or nonlinear optical crystals. For instance, transparent surface-crystallized glasses consisting of $Ba_2TiGe_2O_8$ ferroelectric crystals have been found to exhibit large second-order optical nonlinearities (i.e., ~20 pm/V) comparable to that of $LiNbO_3$ single crystals.[2–6] Transparent crystallized glasses consisting of nonlinear optical nanocrystals have been also fabricated in some glasses.[7–9] At this moment, we have, therefore, many candidates for glass-related fibers with active functions in our hands. Indeed, Iwafuchi *et al.*[10] have succeeded in fabricating nanocrystallized glass fibers showing second harmonic generations (SHGs) in tellurite ($TeO_2$)-based glasses. Drawings of $TeO_2$-based glass fibers including $LiNbO_3$ or $KNbO_3$ crystals have been also tried.[11,12]

In this paper, we focus our attention on the fiber drawing of $BaO-TiO_2-GeO_2$ glasses and the crystallization behavior of fibers. In this study, we succeeded in fabricating transparent crystallized glass fibers with nonlinear optical $Ba_2TiGe_2O_8$ crystals and confirmed from linearly polarized micro-Raman scattering spectra that $Ba_2TiGe_2O_8$ crystals grow from the surface into the center of fibers with keeping high *c*-axis orientations. SHGs were clearly detected from fully crystallized glass fibers.

## II. EXPERIMENTS

The glass composition examined in the present study is $30BaO-15TiO_2-55GeO_2$ (mol %) (designated here as BTG55). As reported in the previous papers,[2–6] BTG55 glass gives the formation of nonlinear optical $Ba_2TiGe_2O_8$ crystals in its crystallization. Commercial powders of reagent grade $BaCO_3$, $TiO_2$, and $GeO_2$ were mixed and melted in a platinum crucible at 1250 °C for 1 h. After melting, the platinum crucible was taken from the furnace, and a silica glass rod with a diameter of 5 cm was put into the melt and pulled up.

a)Author to whom correspondence should be addressed. Tel.: +81 258 47 9313. FAX: +81 258 47 9300.
Electronic mail: komatsu@mst.nagaokaut.ac.jp.

 

The pulling rate of silica rods was ~1 m/s, and glass fibers with a diameter of $\phi$=100–200 $\mu$m and a length of ~1 m were obtained. The temperature of the melt during fiber drawings would be around 1000 °C. In this method, fibers were prepared by a hand-operated technique, but not using any fiber drawing machines. The glass transition $T_g$ and crystallization peak $T_p$ temperatures of glass fibers were determined using differential thermal analyses (DTAs) at a heating rate of 10 K/min.

The glass fibers with a length of 5 cm were heat treated to obtain transparent crystallized glass fibers, and the crystalline phase and orientation of crystals were examined by x-ray diffraction (XRD) analyses using Cu$K\alpha$ radiation and micro-Raman scattering spectrum measurements at room temperature. SHGs of crystallized fibers were examined by measuring second harmonic waves (a wavelength of $\lambda$ =532 nm) for the incident light of a $Q$-switched Nd:YAG (yttrium aluminum garnet) laser with $\lambda$=1064 nm.

## III. RESULTS AND DISCUSSION

### A. Surface crystallization of glass fibers

Transparent glass fibers with $\phi$=100–200 $\mu$m and a few meter length were prepared easily. From polarized optical microscope observations and XRD analyses, it was confirmed that no crystals were included on the surface and in the interior of the fibers. The DTA pattern for fibers ($\phi$ =200 $\mu$m) obtained in this study is shown in Fig. 1, together with the data for bulk (plate) and power samples. Even in the glass fibers, an endothermic peak due to the glass transition and an exothermic peak due to the crystallization are clearly detected, giving the values of $T_g$=678 and $T_p$=823 °C. The large difference in $T_p$ values between fibers and powders suggests that fibers might show a surface crystallization as similar to bulk glasses.[2–6] Furthermore, as the DTA pattern for the fibers is almost the same as that ($T_g$=674 and $T_p$ =834 °C) for the bulk glass, information on the crystallization behavior of bulk glasses clarified in the previous papers[2–6,13] would be applied to the fabrication of transparent crystallized glass fibers. Transparent crystallized glasses with nonlinear optical $Ba_2TiGe_2O_8$ crystals have been fabricated successfully by heat treatments at temperatures of around 690–750 °C for 3 h.[13]

A polarized optical micrograph for the fiber obtained by a heat treatment at 760 °C for 1 h is shown in Fig. 2. It is seen that the crystallization is taking place only on the surface of the fiber, giving the crystalline layer with a thickness of 15 $\mu$m. The micro-Raman scattering spectrum for this crystalline layer is shown in Fig. 3. Several sharp peaks are observed, giving the peaks with strong intensities at 542, 798, 840, and 878 $cm^{-1}$. According to Markgraf *et al.*,[14,15] the peaks at ~542 $cm^{-1}$ are assigned to the symmetric stretching vibrations of O–Ge–O bonds, and the Raman bands at 798, 840, and 878 $cm^{-1}$ correspond to the vibrations in $TiO_5$ units being typical in $Ba_2TiGe_2O_8$ crystals. In the structure of $Ba_2TiGe_2O_8$ crystals, corner-linked $TiO_5$ pentahedra and pyrogermanate groups $Ge_2O_7$ comprise flat sheets perpendicular to the [001] direction, and these sheets are interconnected by tenfold coordinated barium ions.[16–18] The peculiar $Ti^{4+}$ coordination ($TiO_5$) results in permanent electrical dipoles along the [001] direction in the fresnoite-type crystals such as $Ba_2TiGe_2O_8$ and $Ba_2TiSi_2O_8$.[19] The most important feature relating to spontaneous polarizations in

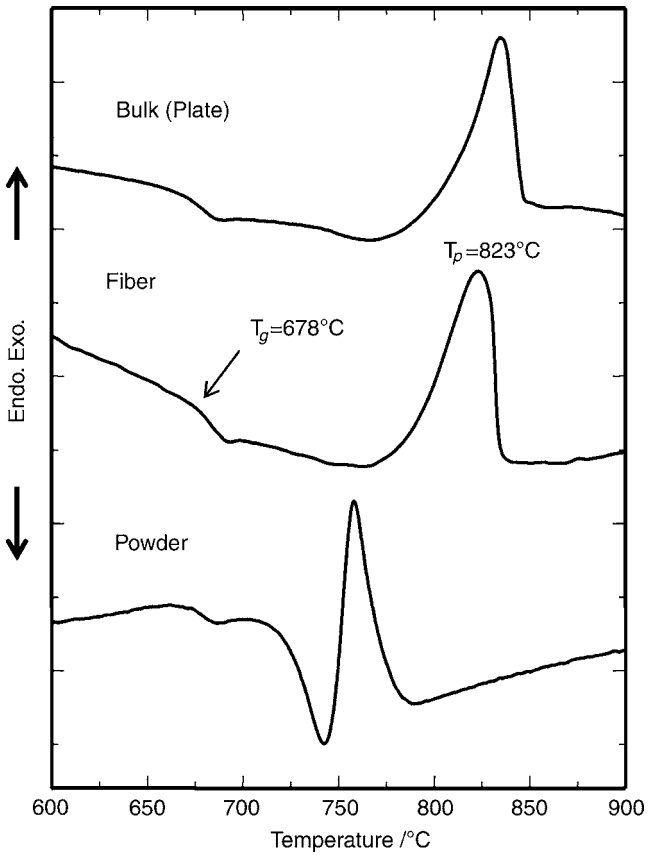


FIG. 1. DTA pattern for fibers with a diameter of $\phi$=200 $\mu$m in $30BaO-15TiO_2-55GeO_2$ glass. The data for bulk (plate) and power samples are also included. $T_g$ and $T_p$ are the glass transition and crystallization peak temperatures, respectively. Heating rate was 10 K/min.

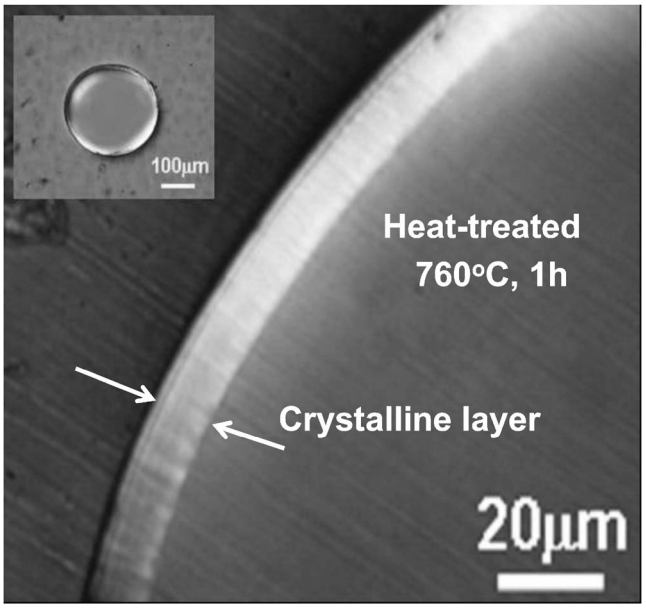


FIG. 2. Polarized optical micrographs for the fiber obtained by a heat treatment at 760 °C for 1 h in $30BaO-15TiO_2-55GeO_2$ glass.

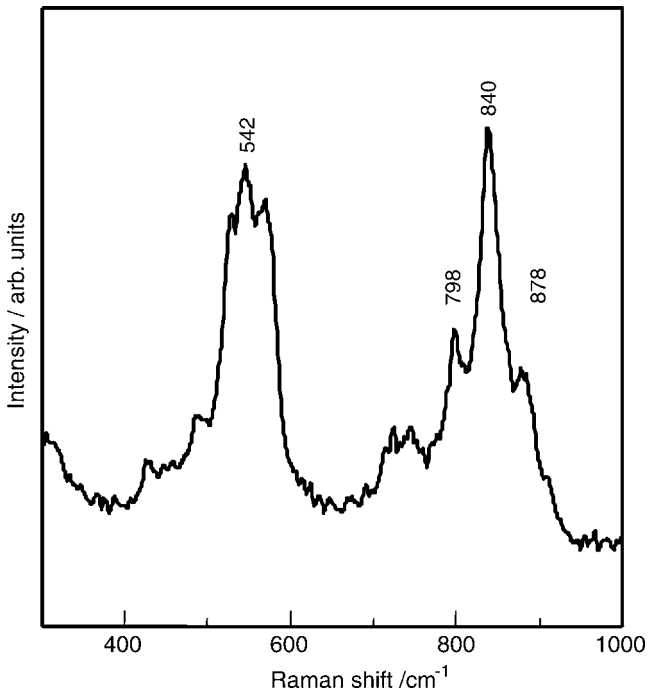


FIG. 3. Micro-Raman scattering spectrum at room temperature for the crystalline layer (Fig. 2) in the fiber obtained by a heat treatment at 760 °C for 1 h in $30BaO-15TiO_2-55GeO_2$ glass.

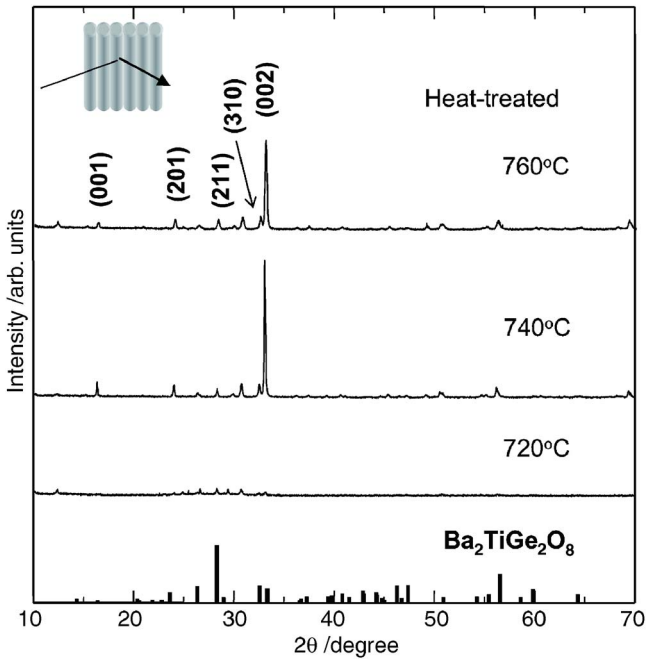


FIG. 4. (Color online) XRD patterns for the bundle of transparent crystallized glass fibers obtained by heat treatments at 720–760 °C for 1 h in $30BaO-15TiO_2-55GeO_2$ glass. The peaks are assigned to $Ba_2TiGe_2O_8$ crystals.

$Ba_2TiGe_2O_8$ crystals is, therefore, the presence of pyramidal $TiO_5$ units.[2,3] Markgraf *et al.*[15] suggested that the Raman bands at 841 and 873 $cm^{-1}$ in $Ba_2TiGe_2O_8$ crystals correspond to the vibrations of Ti–O* in $TiO_5$ polyhedra, and the band at 796 $cm^{-1}$ is related to the basal oxygen-titanium bonds of $Ti-O^-$, where O* denotes the apical oxygen of $TiO_5$ polyhedra. The Raman scattering spectra shown in Fig. 3 indicate, therefore, that the surface crystalline layer in the crystallized glass fiber consists of $Ba_2TiGe_2O_8$ crystals. Furthermore, SHGs were confirmed from the surface crystalline layers in the crystallized glass fibers, demonstrating that $Ba_2TiGe_2O_8$ crystals formed in the crystallized glass fibers are nonlinear optical crystals.

The XRD patterns for the bundle of transparent crystallized glass fibers are shown in Fig. 4. It is also confirmed that $Ba_2TiGe_2O_8$ crystals are formed on the surface. It should be pointed out that the most strong peak corresponds to the (002) plane, suggesting the *c*-axis orientation of $Ba_2TiGe_2O_8$ crystals. The crystal orientation in the crystallized glass fibers will be discussed in the next section in detail.

### B. Crystal orientation in crystallized glass fibers

A polarized optical micrograph for the fiber obtained by a heat treatment at 830 °C for 1 h is shown in Fig. 5. The temperature of 830 °C corresponds to the crystallization peak temperature of $T_p$=823 °C, and thus the fiber is fully crystallized. As can be seen in Fig. 5, a hole is formed at the center of the fiber. It should be pointed out that the formation of holes is frequently observed in fully crystallized glass fibers. The hole formation in the crystallized glass fibers will be discussed in the next section. Here, the orientation of $Ba_2TiGe_2O_8$ crystals in crystallized glass fibers was examined from linearly polarized micro-Raman scattering spectrum measurements, where various configurations about the relationship between the direction of linearly polarized incident laser and the direction of linearly polarized Raman scattering light are possible. The measuring point and the definition of coordinates for the cross section of the crystallized glass fiber are shown in Fig. 5. If $Ba_2TiGe_2O_8$ crystals in the fibers are highly oriented along the crystal growth direction, i.e., along from the surface to the interior, it is expected that the linearly polarized micro-Raman scattering spectra depend strongly on the configuration.

The results for the fully crystallized (830 °C, 1 h) glass fiber are shown in Fig. 6, indicating that the peak profile

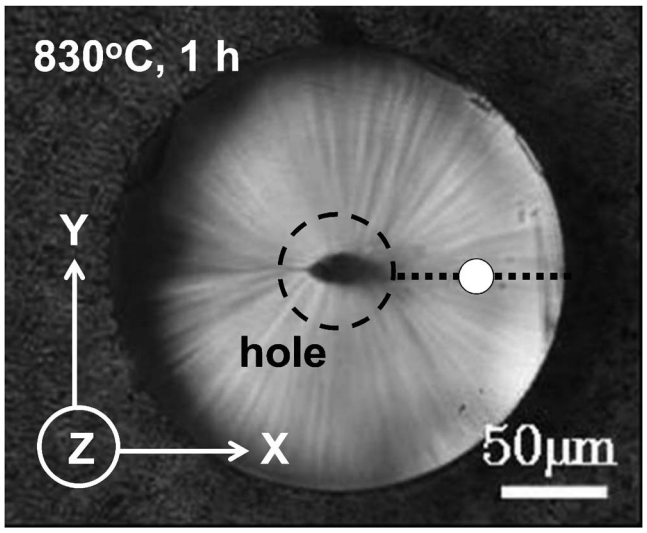


FIG. 5. Polarized optical micrograph for the fiber obtained by a heat treatment at 830 °C for 1 h in $30BaO-15TiO_2-55GeO_2$ glass. A hole is observed at the center of the fiber. The closed circle is a position for linearly polarized micro-Raman scattering spectrum measurements.

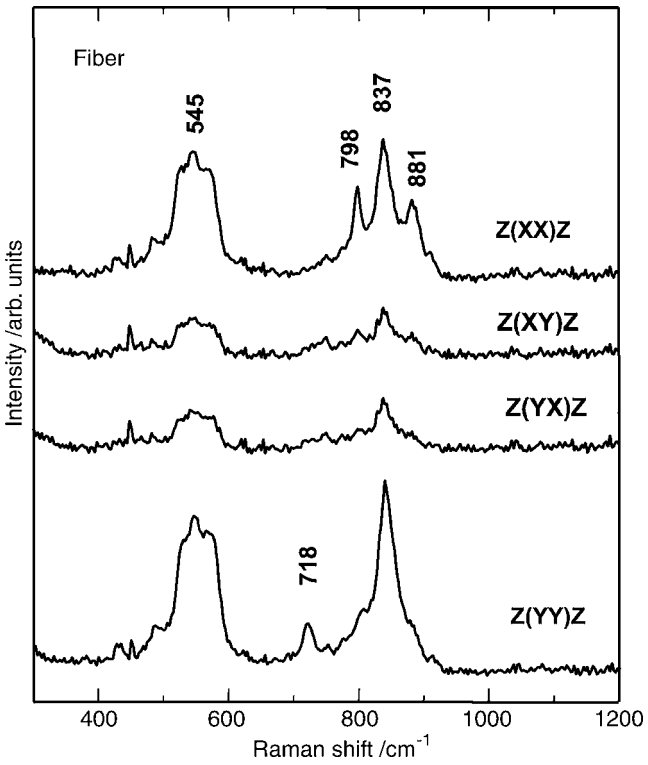


FIG. 6. Linearly polarized micro-Raman scattering spectra for the fiber obtained by a heat treatment at 830 °C for 1 h in $30BaO-15TiO_2-55GeO_2$ glass (Fig. 5).

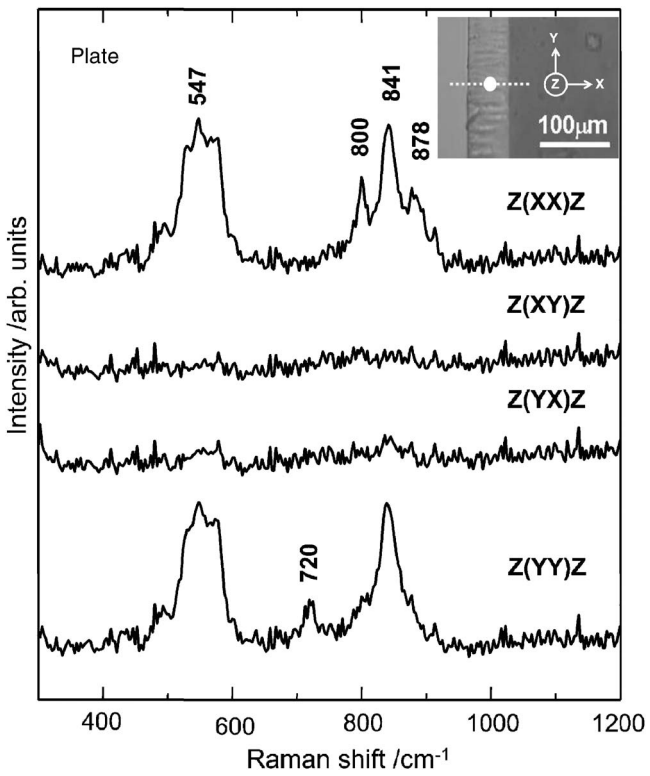


FIG. 7. Linearly polarized micro-Raman scattering spectra for transparent surface-crystallized (bulk) glasses consisting of nonlinear optical $Ba_2TiGe_2O_8$ crystals in $30BaO-15TiO_2-55GeO_2$ glass. The inset is a polarized optical photograph for the surface crystallized sample and the closed circle is a position for measurements.

changes depending on the configuration of polarized micro-Raman scattering measurements. In particular, it should be pointed out that the profile of the Raman bands in the range of 790–900 $cm^{-1}$ in the configuration of $Z(XX)Z$ is largely different from those in the configuration of $Z(YY)Z$. The data shown in Fig. 6 clearly demonstrate that $Ba_2TiGe_2O_8$ crystals in the crystallized glass fibers grow with keeping a crystal growth direction. In the previous papers,[2–5] it has been confirmed that transparent surface-crystallized (bulk) glasses consisting of nonlinear optical $Ba_2TiGe_2O_8$ crystals are fabricated by heat treatments at 720–760 °C and the orientation of the polar $c$-axis in $Ba_2TiGe_2O_8$ crystals occurs from the surface. For the comparison, the linearly polarized micro-Raman scattering spectra for the surface-crystallized (760 °C, 1 h) plate glass are shown in Fig. 7. It is seen that the data (Fig. 7) for the plate glass are almost the same as those (Fig. 6) for the fiber, suggesting that $Ba_2TiGe_2O_8$ crystals in the crystallized glass fiber orient from the surface to the interior, i.e., $c$-axis orientation.

The maps of two-dimensional micro-Raman scattering intensities at the peaks of 720 and 880 $cm^{-1}$ in linearly polarized micro-Raman scattering measurements are shown in Fig. 8. The patterns with the stripe structures are observed, giving the homogeneous intensity in a given direction. These data demonstrate that the $c$-axis orientation of $Ba_2TiGe_2O_8$ crystals is taking place in the whole region of the fully crystallized glass fibers.

### C. Hollow crystallized glass fibers

In the crystallization of glass fibers, holes are formed frequently at the center of fibers. It is of particular interest to clarify the mechanism of the hole formation and to find a technique controlling the hole formation. For this purpose, we checked carefully the behavior of the hole formation in the crystallized fibers, and the following features were found: (1) holes are formed irrespective of fiber diameter, (2) holes tend to form after the crystallization of about 70 vol %, (3) almost all holes have a shape of perfect circle, (4) the diameter of fibers increase about ~5% after crystallization with holes. (5) In the initial stage of the hole formation, many small bubbles and assemblages are observed, as shown in Fig. 9. The above features propose that the main origin of the hole formation in the fully crystallized glass fibers would be due to the precipitation of gasses dissolved into fibers during melt and glass fiber preparations. That is, it is considered that first many small bubbles are generated, then bubbles grow and coagulate, and finally holes are formed at the center of fibers. Gasses of $CO_2$ or $H_2O$ would be expected to be a source of bubbles. This model will be discussed in the next section more in detailed.

Considering the hole formation mechanism and carrying out heat treatments carefully, we succeeded in fabricating transparent crystallized glass fibers with long length holes, i.e., hollow crystallized glass fibers. For example, the optical photograph for the hollow crystallized glass fiber obtained by a heat treatment at 790 °C for 1 h is shown in Fig. 10, where a homogeneous and continuous hole with $\phi=40$ $\mu$m is formed in the fiber with $\phi=200$ $\mu$m. It was confirmed that these long holes exhibit a capillary phenomenon, i.e., water is absorbed up into holes. These transparent hollow crystal-

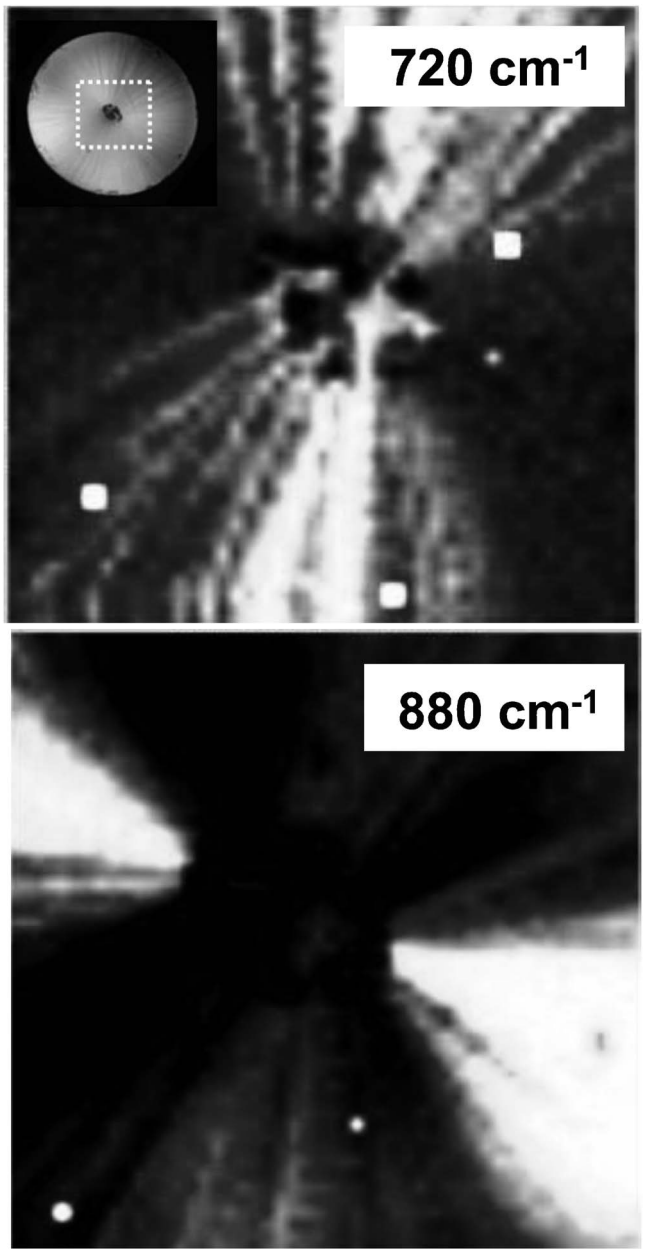


FIG. 8. Maps of two-dimensional micro-Raman scattering intensities at the peaks of 720 and 880 $cm^{-1}$ in linearly polarized micro-Raman scattering measurements for the fiber obtained by a heat treatment at 830 °C for 1 h in $30BaO-15TiO_2-55GeO_2$ glass (Fig. 5). The position for the measurements is around the center.

lized glass fibers having the surface with nonlinear optical $Ba_2TiGe_2O_8$ crystals would have a potential for practical applications in new type active photonic glass fibers.[20]

### D. Crystallized glass fibers without holes

It is also of interest and importance to fabricate transparent crystallized glass fibers without any holes in fiber-type optical device applications. In the field of glass science and technology, $Sb_2O_3$ is well known as an oxide for removing (cleaning) bubbles in melts. In this study, we, therefore, prepared $Sb_2O_3$-added glasses, i.e., $30BaO-15TiO_2-55GeO_2-xSb_2O_3$ glasses with $x=0$, 0.2, 0.4, and 1, where $BaO_2$ (not $BaCO_3$) was used as a raw material for BaO in

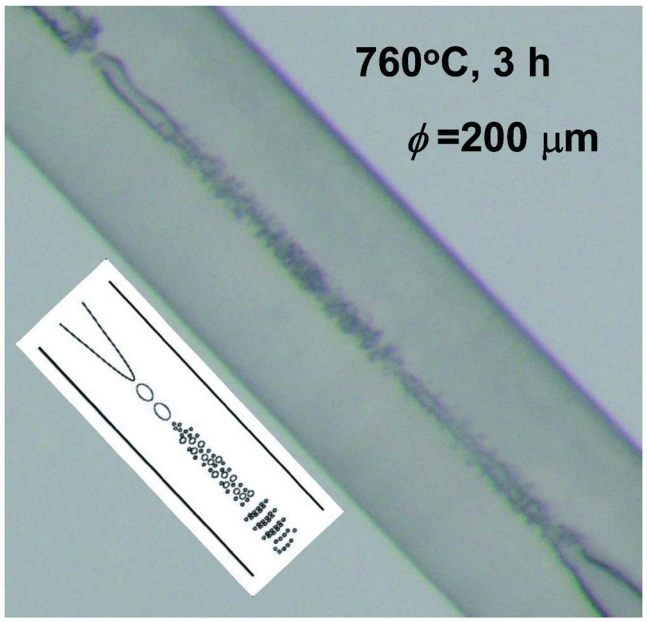


FIG. 9. (Color online) Optical micrograph for the fiber obtained by a heat treatment at 760 °C for 3 h in $30BaO-15TiO_2-55GeO_2$ glass. Many small bubbles and assemblages are present. The inset is an illustration for the bubble formation in the fiber.

order to exclude the possibility of $CO_2$ generation from raw materials. Glass fibers were easily drawn for these compositions and were heat treated at various temperatures to examine the crystallization behavior of fibers. It was confirmed that the glass fibers show the surface crystallization forming $Ba_2TiGe_2O_8$ crystals as similar to the glasses with no addition of $Sb_2O_3$. Furthermore, it was found that the hole formation is largely depressed in $Sb_2O_3$-doped fibers. As an example, optical photographs for the transparent crystallized (770 °C, 3 h) glass fiber obtained by a heat treatment at 770 °C for 1 h in $30BaO-15TiO_2-55GeO_2-0.4Sb_2O_3$ glass are shown in Fig. 11, indicating that the

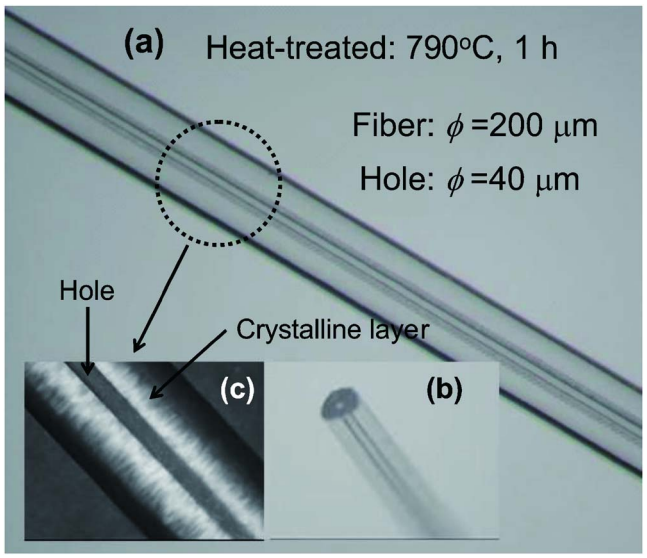


FIG. 10. (Color online) Optical micrographs [(a) and (b)] for the fiber obtained by a heat treatment at 790 °C for 1 h in $30BaO-15TiO_2-55GeO_2$ glass. The inset (c) is a polarized optical micrograph for the fiber.

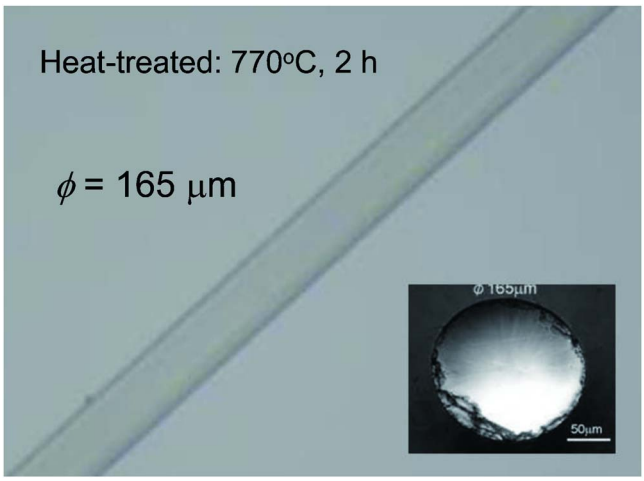


FIG. 11. (Color online) Optical micrograph for the fiber obtained by a heat treatment at 770 °C for 2 h in $30BaO-15TiO_2-55GeO_2-0.4Sb_2O_3$ glass.

crystallization occurs in the whole region of the fiber and no holes are observed even at the center of the fiber. It was also confirmed from linearly polarized micro-Raman scattering spectrum measurements that fully crystallized glass fibers with no holes consist of $Ba_2TiGe_2O_8$ crystals and the *c*-axis orientation of $Ba_2TiGe_2O_8$ crystals is taking place from the surface to the center of fibers.

The SHG microscope observations for the transparent fully crystallized glass fibers with the addition (0.4 mol %) of $Sb_2O_3$ were carried out, and the result with a fiber length of 7.64 mm is shown in Fig. 12, in which *Q*-switched Nd:YAG laser beam with a wavelength of $\lambda=1064$ nm was used and induced SHG emissions ($\lambda=532$ nm) were measured, although the fundamental one ($\lambda=1064$ nm) must be isolated by a cutoff filter before reaching to the charge coupled device for image detection.[21] As can be seen in Fig. 12, the emissions of second harmonic (SH) waves are observed in the whole region of the fiber. It should be point out that the intensity of SH waves in the cross section of the fiber is homogeneous.

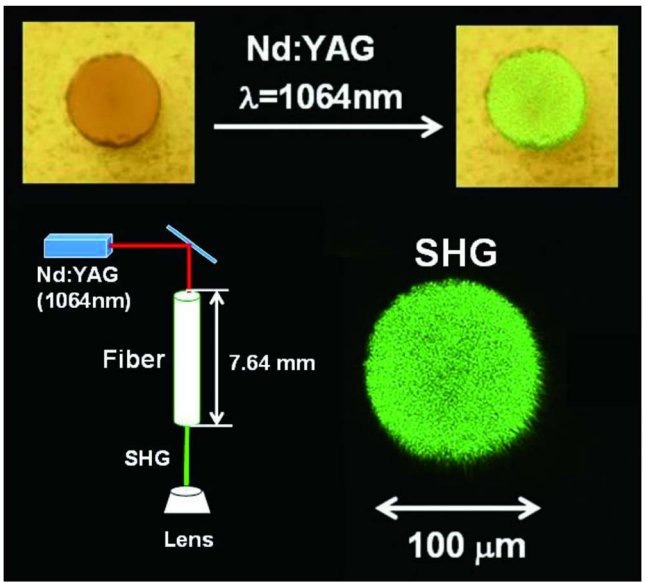


FIG. 12. (Color online) SHG microscope observation for the transparent fully crystallized glass fiber by a heat treatment at 770 °C for 2 h in $30BaO-15TiO_2-55GeO_2-0.4Sb_2O_3$ glass. A fiber length is 7.64 mm.

In previous papers,[22,23] the present authors' group has succeeded in fabricating optically transparent nanocrystallized glass fibers with sharpened tips by using a meniscus chemical etching method in the glass systems of $K_2O-Nb_2O_5-GeO_2$ and $BaO-TiO_2-SiO_2$. Those transparent crystallized glass fibers consist of nanocrystals such as nonlinear optical $Ba_2TiSi_2O_8$, and nanocrystals are formed randomly without any orientations. The present study, therefore, is the first report on the fabrication of transparent crystallized glass fibers consisting of highly oriented nonlinear optical crystals. This kind of fibers would also have a high potential for fiber-type devices with active functions for optical signal processing. Measurements of the efficiency of SH conversions and optical transmission losses at the wavelengths of 1064 and 532 nm are now under consideration.

## IV. CONCLUSION

The glass fibers with a diameter of 100–200 $\mu$m were drawn by just pulling up melts of $30BaO-15TiO_2-55GeO_2$ glass, and transparent crystallized glass fibers consisting of nonlinear optical $Ba_2TiGe_2O_8$ crystals were fabricated by crystallization of glass fibers. It was clarified from linearly polarized micro-Raman scattering spectra that $Ba_2TiGe_2O_8$ crystals grow from the surface to the center of fibers with the *c*-axis orientations. The transparent hollow crystallized glass fibers were fabricated through heat treatments, e.g., fibers with a diameter of $\sim\phi=200$ $\mu$m show hollows (capillary-type holes) with $\sim\phi=40$ $\mu$m. By adding a small amount of $Sb_2O_3$ in glass fiber preparations, transparent crystallized glass fibers with no holes were developed, and SHGs were observed from the fibers. The present study suggests that transparent crystallized glass fibers showing strong SHGs would have a potential for fiber-type light control optical devices.

## ACKNOWLEDGMENTS

This work was supported from the Grant-in-Aid for Scientific Research from the Ministry of Education, Science, Sports, Culture and Technology, Japan, the research collaboration with Asahi Glass Co., Ltd, and by the 21st Century Center of Excellence (COE) Program in Nagaoka University of Technology.

[1] K. Nagashio, A. Watacharapasorn, R. C. DeMattei, and R. S. Feigelson, J. Cryst. Growth **265**, 190 (2004).
[2] Y. Takahashi, Y. Benino, T. Fujiwara, and T. Komatsu, Appl. Phys. Lett. **81**, 223 (2002).
[3] Y. Takahashi, Y. Benino, T. Fujiwara, and T. Komatsu, J. Appl. Phys. **95**, 3503 (2004).
[4] T. Honma, Y. Benino, T. Fujiwara, and T. Komatsu, Appl. Phys. Lett. **88**, 231105 (2006).
[5] H. Masai, T. Fujiwara, Y. Benino, and T. Komatsu, J. Appl. Phys. **100**, 023526 (2006).
[6] N. Toyohara, Y. Benino, T. Fujiwara, S. Tanaka, K. Uematsu, T. Komatsu, and Y. Takahashi, J. Appl. Phys. **99**, 043515 (2006).
[7] R. Sakai, Y. Benino, and T. Komatsu, Appl. Phys. Lett. **77**, 2118 (2000).
[8] G. Senthil, K. B. R. Varma, Y. Takahashi, and T. Komatsu, Appl. Phys. Lett. **78**, 4019 (2001).

[9]Y. Takahashi, K. Kitamura, Y. Benino, T. Fujiwara, and T. Komatsu, Appl. Phys. Lett. **86**, 091110 (2005).
[10]N. Iwafuchi, S. Mizuno, Y. Benino, T. Fujiwara, T. Komatsu, M. Koide, and K. Matusita, Adv. Mater. Res. (N.Y.) **11–12**, 209 (2006).
[11]H. G. Kim, T. Komatsu, R. Sato, and K. Matusita, J. Ceram. Soc. Jpn. **103**, 1073 (1995).
[12]N. S. Prasad, J. Wang, R. K. Pattnaik, H. Jain, and J. Toulouse, J. Non-Cryst. Solids **352**, 519 (2006).
[13]Y. Takahashi, Y. Benino, T. Fujiwara, and T. Komatsu, J. Non-Cryst. Solids **316**, 320 (2003).
[14]S. A. Markgraf, S. K. Sharma, and A. S. Bhalla, J. Am. Ceram. Soc. **75**, 2630 (1992).
[15]S. A. Markgraf, S. K. Sharma, and A. S. Bhalla, J. Mater. Res. **8**, 635 (1993).
[16]T. Höche, W. Neumann, S. Esmaeilzadeh, R. Uecker, M. Lentzen, and C. Rüssel, J. Solid State Chem. **166**, 15 (2002).
[17]K. Iijima, F. Marumo, M. Kimura, and T. Kawamura, Nippon Kagaku Kaishi **10**, 1557 (1981).
[18]T. Höche, C. Rüssel, and W. Neumann, Solid State Commun. **110**, 651 (1999).
[19]P. B. Moore and J. Lousnathan, Science **156**, 1361 (1967).
[20]H. Jelinkova, M. Nemec, J. Sulc, P. Cerny, M. Miyagi, Y. W. Shi, and Y. Matsuura, Prog. Quantum Electron. **28**, 145 (2004).
[21]T. Fujiwara, T. Sawada, T. Honma, Y. Benino, T. Komatsu, M. Takahashi, T. Yoko, and J. Nishii, Jpn. J. Appl. Phys., Part 1 **42**, 7326 (2003).
[22]I. Enomoto, Y. Benino, T. Fujiwara, and T. Komatsu, J. Solid State Chem. **179**, 1821 (2006).
[23]I. Enomoto, Y. Benino, T. Fujiwara, and T. Komatsu, J. Ceram. Soc. Jpn. **115**, 374 (2007).